

Microstructure, optical, and photoluminescence properties of β-Ga_2O_3 films prepared by pulsed laser deposition under different oxygen partial pressures

Rui-Rui Cui(崔瑞瑞), Jun Zhang(张俊), Zi-Jiang Luo(罗子江), Xiang Guo(郭祥), Zhao Ding(丁召), and Chao-Yong Deng(邓朝勇)

Citation: Chin. Phys. B, 2021, 30 (**2**): 028505. DOI: 10.1088/1674-1056/abc164
Journal homepage: http://cpb.iphy.ac.cn; http://iopscience.iop.org/cpb

What follows is a list of articles you may be interested in

Lateral depletion-mode 4H-SiC n-channel junction field-effect transistors operational at 400 ˚C

Si-Cheng Liu(刘思成), Xiao-Yan Tang(汤晓燕), Qing-Wen Song(宋庆文), Hao Yuan(袁昊), Yi-Meng Zhang(张艺蒙), Yi-Men Zhang(张义门), and Yu-Ming Zhang(张玉明)

Chin. Phys. B, 2021, 30 (**2**): 028503. DOI: 10.1088/1674-1056/abc0df

Characteristic enhancement in tunnel field-effect transistors via introduction of vertical graded source

Zhijun Lyu(吕智军), Hongliang Lu(吕红亮), Yuming Zhang(张玉明), Yimen Zhang(张义门), Bin Lu(芦宾), Yi Zhu(朱翊), Fankang Meng(孟凡康), Jiale Sun(孙佳乐)

Chin. Phys. B, 2020, 29 (**5**): 058501. DOI: 10.1088/1674-1056/ab7d99

Experimental and computational study of visible light-induced photocatalytic ability of nitrogen ions-implanted TiO_2 nanotubes

Ruijing Zhang(张瑞菁), Xiaoli Liu(刘晓丽), Xinggang Hou(侯兴刚), Bin Liao(廖斌)

Chin. Phys. B, 2020, 29 (**4**): 048501. DOI: 10.1088/1674-1056/ab6d53

Double superlattice structure for improving the performance of ultraviolet light-emitting diodes

Yan-Li Wang(王燕丽), Pei-Xian Li(李培咸), Sheng-Rui Xu(许晟瑞), Xiao-Wei Zhou(周小伟), Xin-Yu Zhang(张心禹), Si-Yu Jiang(姜思宇), Ru-Xue Huang(黄茹雪), Yang Liu(刘洋), Ya-Li Zi(訾亚丽), Jin-Xing Wu(吴金星), Yue Hao(郝跃)

Chin. Phys. B, 2019, 28 (**3**): 038502. DOI: 10.1088/1674-1056/28/3/038502

Preparation of Ga_2O_3 thin film solar-blind photodetectors based on mixed-phase structure by pulsed laser deposition

Y M Lu(吕有明), C Li(李超), X H Chen(陈相和), S Han(韩瞬), P J Cao(曹培江), F Jia(贾芳), Y X Zeng(曾玉祥), X K Liu(刘新科), W Y Xu(许望颖), W J Liu(柳文军), D L Zhu(朱德亮)

Chin. Phys. B, 2019, 28 (**1**): 018504. DOI: 10.1088/1674-1056/28/1/018504

Microstructure, optical, and photoluminescence properties of β-Ga_2O_3 films prepared by pulsed laser deposition under different oxygen partial pressures*

Rui-Rui Cui(崔瑞瑞)[1], Jun Zhang(张俊)[2], Zi-Jiang Luo(罗子江)[1], Xiang Guo(郭祥)[1], Zhao Ding(丁召)[1], and Chao-Yong Deng(邓朝勇)[1,†]

[1] *Power Semiconductor Device Reliability Center of the Ministry of Education, Department of Electronic Science, College of Big Data and Information Engineering, Guizhou University, Guiyang* 550025, *China*

[2] *College of Computer and Information Engineering, Guizhou University of Commerce, Guiyang* 550014, *China*

(Received 24 August 2020; revised manuscript received 21 September 2020; accepted manuscript online 15 October 2020)

The β-Ga_2O_3 films are prepared on polished Al_2O_3 (0001) substrates by pulsed laser deposition at different oxygen partial pressures. The influence of oxygen partial pressure on crystal structure, surface morphology, thickness, optical properties, and photoluminescence properties are studied by x-ray diffraction (XRD), atomic force microscope (AFM), scanning electron microscope (SEM), spectrophotometer, and spectrofluorometer. The results of x-ray diffraction and atomic force microscope indicate that with the decrease of oxygen pressure, the full width at half maximum (FWHM) and grain size increase. With the increase of oxygen pressure, the thickness of the films first increases and then decreases. The room-temperature UV-visible (UV-Vis) absorption spectra show that the bandgap of the β-Ga_2O_3 film increases from 4.76 eV to 4.91 eV as oxygen pressure decreasing. Room temperature photoluminescence spectra reveal that the emission band can be divided into four Gaussian bands centered at about 310 nm ($\sim$ 4.0 eV), 360 nm ($\sim$ 3.44 eV), 445 nm ($\sim$ 2.79 eV), and 467 nm ($\sim$ 2.66 eV), respectively. In addition, the total photoluminescence intensity decreases with oxygen pressure increasing, and it is found that the two UV bands are related to self-trapped holes (STHs) at O1 sites and between two O2-s sites, respectively, and the two blue bands originate from V_{Ga}^{2-} at Ga1 tetrahedral sites. The photoluminescence mechanism of the films is also discussed. These results will lay a foundation for investigating the Ga_2O_3 film-based electronic devices.

Keywords: β-Ga_2O_3, pulsed laser deposition, band gap, photoluminescence

PACS: 85.60.Gz, 81.15.Fg, 81.10.Pq **DOI:** 10.1088/1674-1056/abc164

1. Introduction

The transparent semiconductor material of β-Ga_2O_3, which has wider direct band gap ($\sim$ 4.9 eV), prominent chemical properties and thermal stability, can be used as a required research material in the future ultraviolet, deep ultraviolet optoelectronic devices, and high-frequency and high-power devices, and thus has attracted much attention in recently years.[1–6] The β-Ga_2O_3 thin films have been prepared by molecular beam epitaxy,[7] metal–organic chemical vapor deposition,[8] pulsed laser deposition (PLD),[9] radio frequency (RF) magnetron sputtering,[10] vacuum thermal evaporation,[11] *etc*. Among these means, the PLD is more helpful in obtaining the high-quality metal oxide films due to its several advantages, such as the good control of the stoichiometry, resulting energetic materials, compatibility with background pressure, and easy control of growth temperature and oxygen pressure during preparation. The materials used as substrates for depositing β-Ga_2O_3 epitaxial thin films include Ga_2O_3, Al_2O_3, Si, GaN substrate, *etc*.[9,12,13] Due to the cheap price and reliable technical indexes of the Al_2O_3 and Si substrate used in many industrial applications, most of the reported β-Ga_2O_3 epitaxial films are heteroepitaxial films.

The quality of β-Ga_2O_3 epitaxial films is the key to semiconductor light-emitting devices and transparent electronic devices. The structure and properties of β-Ga_2O_3 films could be affected by substrate, process and parameters. According to previous reports, some considerable changes in microstructure, optical properties, photoluminescence (PL) properties, etc. for β-Ga_2O_3 films deposited on *c*-plane sapphire substrate at different oxygen partial pressures by PLD have been studied.[14–18] Wang reported the effect of oxygen pressure on microstructure of β-Ga_2O_3 film prepared by PLD, and obtained the $(\bar{2}01)$-oriented epitaxial thin films on *c*-sapphire substrate.[19] Chen *et al*.[20] and Lu *et al*.[21] reported the deposition orientation, UV absorption spectra, and the UV response characteristics of the β-Ga_2O_3 films prepared by PLD. Vu *et al*. found that the conductance and the energy band gap of β-Ga_2O_3 thin films could be controlled by oxygen partial pressure.[14] Zhang *et al*. investigated the influence of

*Project supported by the Guizhou Provincial Science and Technology Planning Project, China (Grant No. 2018-5781), the National Natural Science Foundation of China (Grant No. 51762010), the Guizhou Provincial Science and Technology Foundation, China (Grant Nos. 2020-1Y021 and 2020-1Y271), and the Guizhou Provincial High-level Innovative Talents, China (Grant No. 2018-4006).

†Corresponding author. E-mail: cydeng@gzu.edu.cn

© 2021 Chinese Physical Society and IOP Publishing Ltd

oxygen pressure on the structural, optical transmission spectra and electrical properties.[22] Tak *et al*. studied the effect of point defects on the work function of β-Ga_2O_3 film prepared by PLD through controlling the growth pressure.[23] Liu *et al*. reported the structure and photoluminescence properties of β-Ga_2O_3 thin films prepared by PLD through changing oxygen pressure and analyzed their luminescence origin.[15] However, to date, the systematic researches about the influence of oxygen partial pressure on microstructure, thickness, optical properties, and photoluminescence properties of β-Ga_2O_3 films have rarely been reported. Thus, in this work, we use the PLD to grow the Ga_2O_3 films on Al_2O_3 (0001) substrates under various oxygen partial pressures at 780 °C, and systematically investigate the influence of oxygen partial pressure on crystal structure, surface morphology, thickness, optical properties, and photoluminescence properties of β-Ga_2O_3 thin films through x-ray diffraction (XRD), atomic force microscope (AFM), scanning electron microscope (SEM), spectrophotometer, and spectrofluorometer. Meantime, we also discuss the mechanism of photoluminescence of β-Ga_2O_3 thin films.

2. Experiment

Ga_2O_3 films were prepared by a PLD on Al_2O_3 substrates (0001), where a KrF excimer laser source ($\lambda = 248$ nm) was used. The Ga_2O_3 ceramic target was synthesized by a solid-state reaction method. The Ga_2O_3 films were deposited at 780 °C in the PLD system, with a repetition frequency of 3 Hz and the oxygen partial pressure of 10, 1, 0.2, and 0.0004 Pa, respectively. The energy density of the pulsed laser for the deposition was about 3 J/cm^2. The Al_2O_3 substrate was placed parallel to and at 45 cm far from the target. The target rotates uniformly during the growth. The films were deposited for about 40 min at different oxygen pressure and then, *in-situ* annealed for 30 min in a 2000-Pa O_2 atmosphere.

The crystal structure for each of the films was characterized by x-ray diffractometer with Cu K radiation (D/Max-RA, Rigaku, $\lambda = 1.5418$ Å) at a scanning speed of 2 °/min in steps of 0.02°. The surface morphologies of the films were recorded by an atomic force microscope (Bruker Multimode 8). The thickness of β-Ga_2O_3 layer was measured by scanning electron microscope (Regulus8100, Hitachi). The UV-visible (UV-Vis) absorption spectra were recorded on a spectrophotometer (U4100, HORIBA). The PL spectra were obtained with a HORIBA FluoroMax-4 spectrofluorometer equipped with a 150-W xenon lamp as an excitation source. All the measurements were carried out at room temperature.

3. Results and discussion

Figure 1 shows the XRD patterns of the Ga_2O_3 films deposited on Al_2O_3 (0001) substrates with oxygen partial pressure ($p(O_2) = 10$, 1, 0.2, and 0.0004 Pa) at 780 °C. As can be seen, besides the diffraction peak of the Al_2O_3 substrate (0006), the diffraction peaks at about 18.8°, 38.2°, and 59.2° can be observed clearly in each of all the films, which can be assigned to the $(\bar{2}01)$, $(\bar{4}02)$, and $(\bar{6}03)$ lattice planes of the monoclinic β-Ga_2O_3 (JCPDS file No. 41-1103), respectively, demonstrating the polycrystalline nature of the films. When the films are deposited at the oxygen partial pressures of 10 Pa and 1 Pa, besides the aforementioned diffraction peaks, the (400), $(\bar{6}01)$, and $(\bar{8}01)$ lattice planes of β-Ga_2O_3 located at about 30.2°, 44.3°, and 59.8° are observed. And with the decreasing of oxygen partial pressure, the (400), $(\bar{6}01)$, and $(\bar{8}01)$ lattice plane disappear, and a single oriented β-Ga_2O_3 film grown parallel to its $(\bar{2}01)$ crystal plane is formed on the c-sapphire substrate at a relatively low oxygen partial pressure. Moreover, the intensities of the main diffraction peaks first increase and then decrease, indicating that the best crystallization of the film can be obtained under an oxygen pressure of 0.2 Pa.

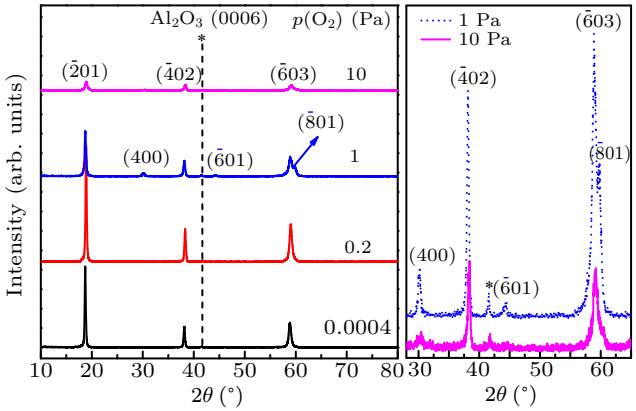


Fig. 1. XRD patterns of Ga_2O_3 films deposited on Al_2O_3 substrates (0001) under different oxygen partial pressures.

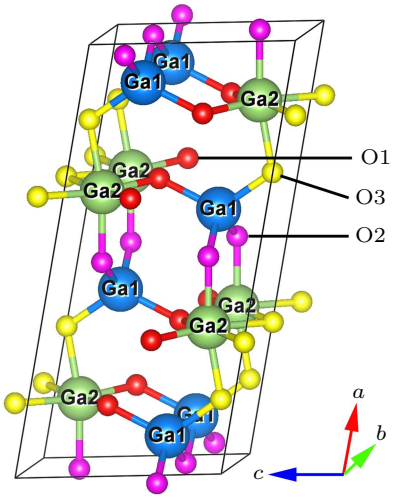


Fig. 2. Crystal structure of β-Ga_2O_3.

The crystal structure of β-Ga_2O_3 is given in Fig. 2. The β-Ga_2O_3 crystallizes into monoclinic structure, and its cell parameters are as follows: $a = 12.23$ Å, $b = 3.04$ Å, $c = 5.80$ Å, $\alpha = \gamma = 90°$, and $\beta = 103.8°$, and the space group is $C2/m$.[24]

It can be observed in Fig. 2 that Ga atom occupies two lattice sites: [Ga1] that has tetrahedrally coordination, and [Ga2] that has octahedral coordination. There are three O sites in the structure: three-fold coordinated O1, three-fold coordinated O2, and four-fold coordinated O3 sites. Thus, β-Ga_2O_3 crystal cell is composed of two GaO_4 tetrahedra and two edge-sharing GaO_6 octahedra.[21] The (400) crystal plane is on the upper surface of the β-Ga_2O_3 cell, and the $(\bar{4}02)$ crystal plane is an oblique plane composed of O or Ga atoms of an octahedral in vitro triangle. Moreover, the $(\bar{2}01)$ crystal plane is parallel to the $(\bar{4}02)$ and their atomic arrangements are the same. As is well known, the larger the dangling bond density on the surface of a crystal plane, the greater the attraction to the reaction atoms is, so that the reaction atomic energy with less migration energy migrates to the crystal plane surface; similarly, if the dangling bond density on a crystal plane surface is smaller, the force to attract the reaction atoms is weak, and only the atoms with larger migration energy can migrate to the surface of that type of crystal plane. Chen *et al.* have pointed out that the surface of (400) crystal plane of β-Ga_2O_3 has a higher density of suspended bonds than that of surface $(\bar{2}01)$, thus, the (400) crystal plane of β-Ga_2O_3 is more attractive to Ga and O atoms and requires less energy for the migration of reactive atoms.[20] Therefore, the (400) and $(\bar{2}01)$ orientation of β-Ga_2O_3 can be obtained under high oxygen pressure under which the migration energy of reactive atoms is lower. Meantime, some Ga atoms or O atoms do not even have enough energy to migrate to the surface of (400) crystal plane of β-Ga_2O_3, and these reaction atoms can migrate to other crystal planes which are less attractive to the reaction atoms as $(\bar{6}01)$ and $(\bar{8}01)$ lattice planes of β-Ga_2O_3 are under 1-Pa and 10-Pa oxygen pressure conditions, which shows multi-orientation growth. However, when the oxygen pressure is 10 Pa, all the diffraction peaks intensities are weak due to the very low migration energy of reactive atoms. The lower the oxygen pressure, the higher the migration energy of the reaction atoms is and the more the $(\bar{2}01)$-direction β-Ga_2O_3 is deposited. As shown in Fig. 1, when the oxygen partial pressure is at 0.0004 Pa and 0.2 Pa, the high-quality $(\bar{2}01)$-oriented epitaxial β-Ga_2O_3 films can be successfully grown on the c-sapphire substrates.

According to Fig. 1, the full width at half maximum (FWHM) values of $(\bar{2}01)$ diffraction peak at oxygen partial pressure of 10, 1, 0.2, and 0.0004 Pa are 0.470°, 0.314°, 0.251°, and 0.251°, respectively. According to Scherrer's formula, the average grain size of β-Ga_2O_3 films can be estimated from the following equation:

$$D = \frac{0.9 \cdot \lambda}{\beta \cdot \cos\theta}, \tag{1}$$

where D, λ, β, and θ are the average grain size, the wavelength of x rays, the half-peak width of the diffraction peak, and the diffraction angle of Bragg diffraction when tested for 2θ, respectively. The values of D are calculated as indicated in Table 1. As can be seen, with the decreasing of oxygen pressure, the average grain size of β-Ga_2O_3 films increases.

Table 1. Average crystallite size (D in unit nm) calculated from x-ray diffraction patterns and RMS roughness of β-Ga_2O_3 films deposited under different oxygen pressures.

Oxygen partial pressure (Pa)	Average crystallite size D (nm)	RMS roughness
10	17.0	2.83
1	25.5	1.77
0.2	31.9	2.58
0.0004	31.9	2.52

Figures 3(a)–3(d) show the surface morphologies and cross-sectional images of β-Ga_2O_3 films grown at the oxygen pressure of 10, 1, 0.2, 0.0004 Pa, respectively. The root mean square (RMS) values of roughness are also given in Table 1. The scan range is 2 μm ×2 μm. It can be seen that the island-like structures appear in all samples, and the surfaces of all films are uniform. In addition, the surface morphology is dependent on the oxygen partial pressure during growth. With the decrease of oxygen partial pressure, the grain size increases, which is consistent with the calculation result of XRD. The particle sizes of the film grown at the oxygen pressure of 10 Pa are much smaller. When the oxygen partial pressure reaches to 0.2 Pa, both large and small particles are randomly present in the film. When the oxygen partial pressure reaches to 0.0004 Pa, no obvious change in grain size is found, which is consistent with the XRD results. As is well known, when the oxygen pressure is high, the plasma produced by laser irradiation will collide with the oxygen molecules in the cavity many times during the transport in space and will lose some of its energy, thus, the migration energy of the surface adsorption atoms decreases. The adsorption atoms can nucleate on the substrate surface, but many adsorption atoms cannot be combined with each other, that is, only the adsorption atoms near the nucleus can be transferred to the nucleus and contribute to the crystallization, so the particle size is smaller. When the oxygen partial pressure decreases, the collision between laser plasma and oxygen molecules is bound to decrease, which reduces the energy loss of particles, thus facilitating the diffusion on the substrate surface. In addition, substrate heating also provides the necessary energy for atoms diffusion. Therefore, the mobility of the adsorbed atoms increases, more adsorbed atoms move to the nucleus, and the nearby structure begins to bind, leading to the grain size to increase. In addition, the maximum of the RMS roughness is 2.83 nm, indicating that the surfaces of obtained films are smooth.

The cross-section of the β-Ga_2O_3 films grown at different oxygen pressures are shown in the insets of Fig. 3, respectively. When the oxygen partial pressure increases from 0.0004 Pa to 1 Pa, the thickness values of the β-Ga_2O_3 films

increase from 90 nm to 202 nm. But when the oxygen pressure continues to increase to 10 Pa, the thickness values of the β-Ga_2O_3 films decrease to 152 nm. This may be due to the fact that when the oxygen partial pressure continues to increase, the decrease of the migration energy of reactive Ga and O atoms can reduce the thickness of the β-Ga_2O_3 films. As can be seen from the XRD results, when the oxygen partial pressure increases from 0.0004 Pa to 1 Pa, the β-Ga_2O_3 films grown mainly parallel to $(\bar{2}01)$ orientations. And the increase of oxygen pressure leads oxygen to be enriched on the substrate surface. Meantime, the O-rich condition is beneficial to the growth of $(\bar{2}01)$ β-Ga_2O_3.[20] The effect of increasing oxygen pressure on the increase in thickness of the β-Ga_2O_3 film exceeds the effect of the decrease of the thickness induced by reducing the migration energy of reactive atoms, thereby leading the thickness values of the β-Ga_2O_3 films to increase.

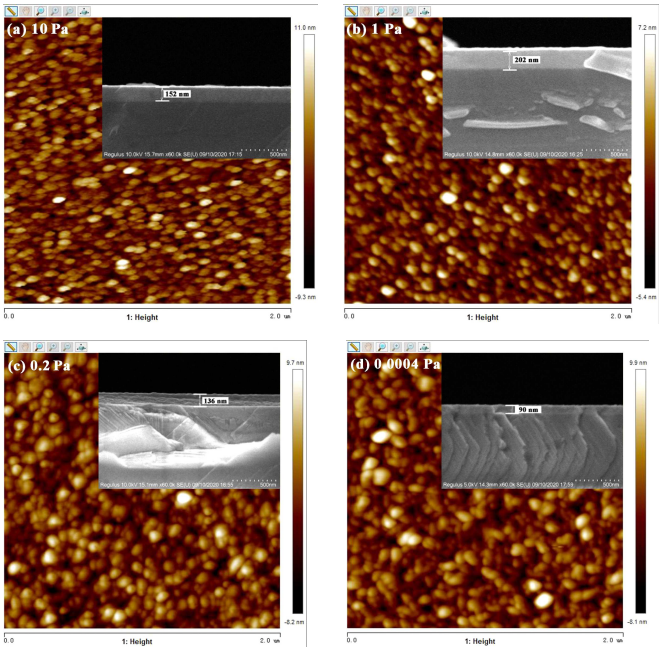


Fig. 3. AFM images of β-Ga_2O_3 films deposited under different oxygen pressures, with insets showing SEM cross-sectional images.

The room-temperature UV-Vis absorption spectra of β-Ga_2O_3 films deposited at various oxygen partial pressures at 780 °C are shown in Fig. 4(a). An absorption edge of β-Ga_2O_3 film is observed at about 275 nm when the oxygen pressure is 10 Pa. While the absorption band edge moves toward the shorter wavelength direction with the decreasing of oxygen pressure. When the oxygen partial pressure decreases to 0.0004 Pa, the absorption band edge decreases to 269 nm. As is well known, the Ga_2O_3 has been proved to be a direct band gap material, the optical band gap (E_g) can be evaluated according to the relationship: $(\alpha h\nu)^2 \propto (h\nu - E_g)$, where $h\nu$ is the incident photon energy, α is the absorbance coefficient.[25,26] The E_g of β-Ga_2O_3 film is obtained by extrapolating the linear portion of the plot of $(\alpha h\nu)^2$ *versus* energy ($h\nu$) as demonstrated in Fig. 4(b). The inset of Fig. 4(b) shows the dependence of bandgap of β-Ga_2O_3 films on oxygen partial pressure. As can be seen, the bandgap of the β-Ga_2O_3 film increases from 4.76 eV to 4.91 eV with the oxygen partial pressure decreasing. The films exhibit shorter absorption edge of about 4.88 eV and 4.91 eV at lower oxygen partial pressure of 0.2 Pa and 0.0004 Pa, respectively. The result is consistent with the literature data.[14,27] Similarly, it is reported that the direct band gap of ITO film is blue-shifted with the decrease of oxygen partial pressure, which is due to the carrier concentration decreasing by Burstein–Moss displacement.[28] In addition, the band gap of the film grown at 0.2 Pa is 4.88 eV, which is consistent with the reported result for Ga_2O_3 bulk ($\sim$ 4.9 eV).[29,30]

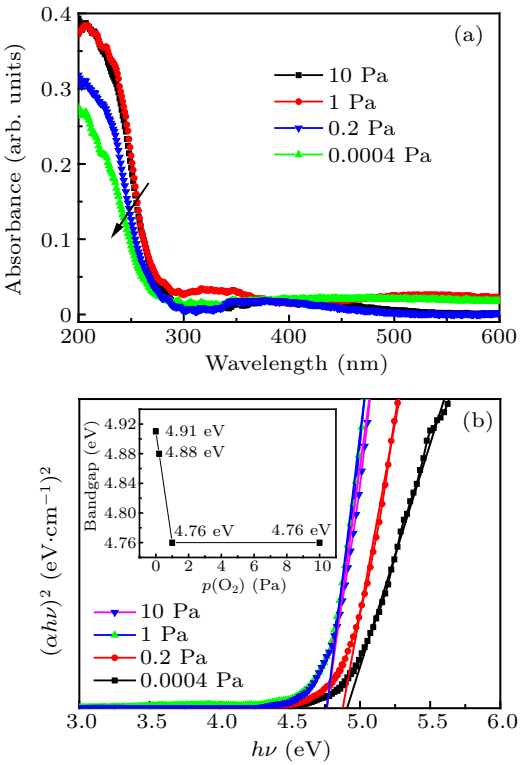


Fig. 4. (a) UV-Vis absorption spectra of β-Ga_2O_3 films deposited under different oxygen partial pressures, and (b) band gap calculation plot of β-Ga_2O_3 films, with inset showing dependence of bandgap on oxygen partial pressure.

The PL spectra of β-Ga_2O_3 films excited at 255 nm (4.86 eV), grown in 10, 1, 0.2, and 0.0004 Pa, respectively, are given in Fig. 5(e). The PL spectra of the β-Ga_2O_3 films exhibit a strong, broad, and asymmetric emission band from 270 nm to 490 nm which is located in the UV and blue light region. The total PL intensity decreases with the increase of the oxygen partial pressure, which indicates that the oxygen partial pressure has a quenching effect on the PL intensity, which is consistent with the results reported by Liu *et al.*[15] and Feng *et al.*[17] From the above observation, it is considered that with the increase of oxygen pressure, defects and dislocations in the films increase, and these defects will degrade the quality of films, and the increase of non-radiative recombination process related to defects will lead the PL intensity to decrease.[17] To investigate the origin of the emission bands of β-Ga_2O_3 films, figures 5(a)–5(d) display the Gaussian fitting peaks of

the spectra of β-Ga_2O_3 films grown under 10, 1, 0.2, and 0.0004 Pa, respectively. It can be seen that the four Gaussian bands are centered at about 310 ($\sim$ 4.0 eV), 360 ($\sim$ 3.44 eV), 445 ($\sim$ 2.79 eV), and 467 nm ($\sim$ 2.66 eV), respectively. As is well known, the photoluminescence of the Ga_2O_3 is ascribed to the recombination of electrons in the donor band with holes in the acceptor band which is formed by the internal defects of film.[31,32] According to previous reports, the UV emission is attributed to an intrinsic phenomenon of self-trapped holes' (STHs') recombination independent of sample experience and dopant property.[33,34] The blue light emission may result from the tunneling-trapped recombination of an electron in the donor band (V_O) and a hole in the acceptor band, the acceptor band can be formed by gallium vacancy (V_{Ga}), or a charged gallium-oxygen vacancy pair (V_O; V_{Ga}).[33,35] According to theoretical calculation and experimental investigations, the UV emission band centered at 310 nm ($\sim$ 4.0 eV) may be attributed to STHs in a small polaron state since this defect-related energy level derives from O1 sites, which has the lower formation energy than the other intrinsic defects in O-poor β-Ga_2O_3 layers.[16,36,37] The other UV band at about 360 nm ($\sim$ 3.44 eV) originates from the recombination of electrons with STHs in a small polaron state between two O2-s sites.[16,36] The two blue emission bands centered at about 445 nm ($\sim$ 2.79 eV) and 467 nm ($\sim$ 2.66 eV) nm are considered to originate from gallium vacancies in the (2-) charge state (V_{Ga}^{2-}) at Ga1 tetrahedral sites.[16,36] Therefore, the UV emission band ($\sim$ 4.0 eV), ($\sim$ 3.44 eV), and two blue emission bands ($\sim$ 2.79 eV and 2.66 eV) are considered to come from the recombination with STHs at O1 sites, STHs between two O2-s sites and V_{Ga}^{2-} at Ga1 tetrahedral sites, respectively.

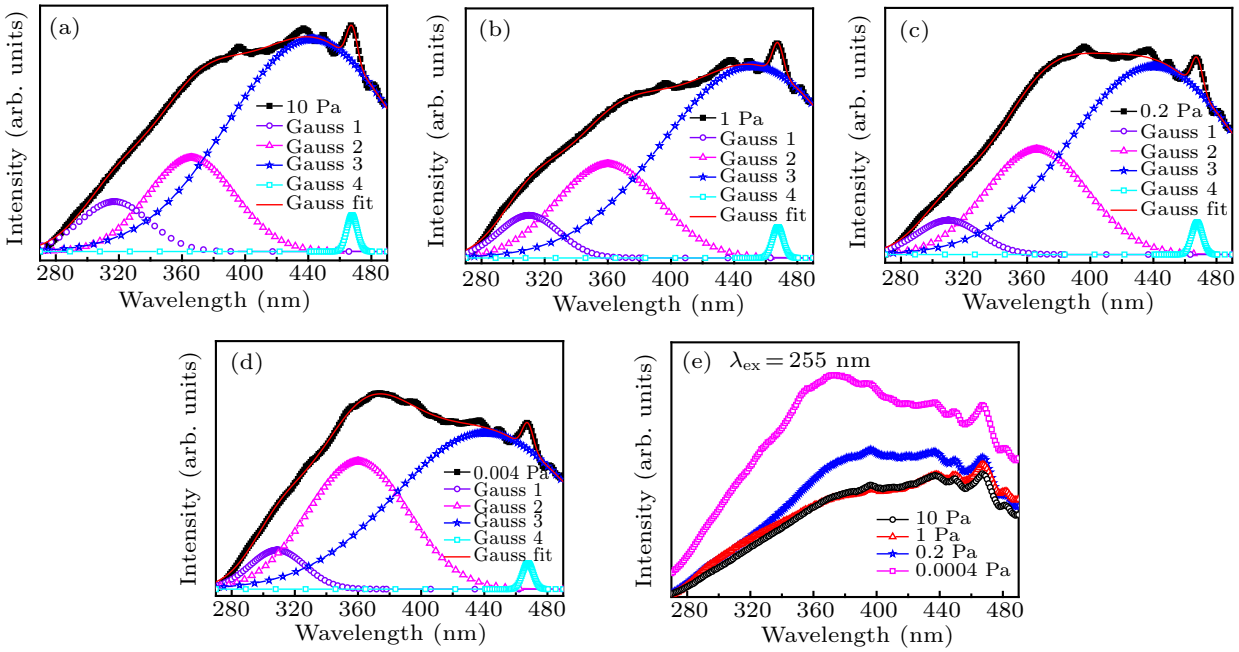


Fig. 5. (a)–(d) Gaussian fitting peaks of PL spectra of β-Ga_2O_3 films grown under 10, 1, 0.2, and 0.0004 Pa, respectively, and (e) room temperature PL spectra of β-Ga_2O_3 films.

Table 2. Detailed peak fitting data of PL.

Samples	Fit peak	Peak center (nm)	Energy (eV)
O_2: 10 Pa	Gauss 1	315	3.94
	Gauss 2	365	3.40
	Gauss 3	442	2.81
	Gauss 4	467	2.66
O_2: 1 Pa	Gauss 1	310	4.00
	Gauss 2	360	3.44
	Gauss 3	450	2.76
	Gauss 4	467	2.66
O_2: 0.2 Pa	Gauss 1	310	4.00
	Gauss 2	365	3.40
	Gauss 3	440	2.82
	Gauss 4	467	2.66
O_2: 0.0004 Pa	Gauss 1	310	4.00
	Gauss 2	360	3.44
	Gauss 3	445	2.79
	Gauss 4	467	2.66

Figure 6 gives a simple mechanism model of the PL of β-Ga_2O_3 film in UV and blue light region. When excited by the 255-nm light, the electrons absorb the energy and then jump to shallow donor levels below the conduction band from acceptor defect levels above the valence band.[18,38] In the β-Ga_2O_3, the electrons can be thermally excited into the conduction band from these shallow donor levels. The electrons are in an unstable state and can move freely in the conduction band and recombine with holes by self-trapping and thus emitting the UV light. A trapped electron in the donor band can realize the radiative recombination with a trapped hole in the acceptor band through tunnel-capture and then emit the blue light. Based on previous analysis, the four emission bands are attributed to three defects in β-Ga_2O_3 film: the two UV bands come from STHs at O1 site ($\sim$ 4.0 eV) and between two O2-s

sites ($\sim$ 3.44 eV), respectively, the origins of two blue bands ($\sim$ 2.79 eV and 2.66 eV) are V_{Ga}^{2-} at Ga1 tetrahedral sites.

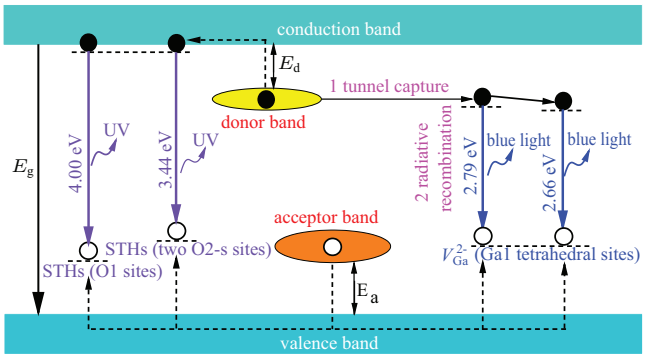


Fig. 6. Mechanism model of PL of β-Ga_2O_3 film in UV and blue regions.

4. Conclusions

In this work, the effect of oxygen partial pressure on the microstructures, thickness, optical properties, and photoluminescence properties of β-Ga_2O_3 films deposited on Al_2O_3 substrate (0001) by PLD are investigated. The XRD and AFM results show that the film deposited at an oxygen pressure of 0.2 Pa has the best crystallinity and surface morphology. With the decrease of oxygen pressure, the bandgap of the β-Ga_2O_3 films increases from 4.76 eV to 4.91 eV. The photoluminescence spectra contain a strong, broad, and asymmetric emission band from 270 nm to 490 nm located in the UV and blue light region and can be divided into four Gaussian fitting peaks. The UV and blue bands are related to STHs at O1 sites and between two O2-s sites, and V_{Ga}^{2-} at Ga1 tetrahedral sites.

Acknowledgment

We would like to thank Dr. Kaixin Guo and Guobin Ma for the test of Ga_2O_3 films.

References

[1] Zhang J Y, Shi J L, Qi D C, Chen L and Zhang K H L 2020 *APL Mater.* **8** 020906
[2] Higashiwaki M, Sasaki K, Murakami H, Kumagai Y, Koukitu A, Kuramata A, Masui T and Yamakoshi S 2016 *Semicond. Sci. Tech.* **31** 034001
[3] Rath P, Ummethala S, Nebel C and Pernice W H P 2015 *Phys. Status Solidi (a)* **212** 2385
[4] Nikolaev V I, Maslovc V, Stepanov S I, Pechnikov A I, Krymov V, Nikitin I P, Guzilova L I, Bougrov V E and Romanov A E 2017 *J. Cryst. Growth* **457** 132
[5] Yu X W, Cui H Y, Zhu M D, Xia Z L and Sai Q L 2019 *Chin. Phys. B* **28** 077801
[6] Hoshikawa K, Ohba E, Kobayashi T, Yanagisawa J, Miyagawa C and Nakamura Y 2016 *J. Cryst. Growth* **447** 36
[7] Kalarickal N K, Xia Z B, McGlone J, Krishnamoorthy S, Moore W, Brenner M, Arehart A R, Ringe S A and Rajan S 2019 *Appl. Phys. Lett.* **115** 152106
[8] Yang X K, Du X J, He L N, Wang D, Zhao C C, Liu J, Ma J and Xiao H D 2020 *J. Mater. Sci.* **55** 8231
[9] Rafique S, Han L, Tadjer M J, Freitas J A, Mahadik N A and Zhao H P 2016 *Appl. Phys. Lett.* **108** 182105
[10] Zhang Y F, Chen X H, Xu Y, Ren F F, Gu S L, Zhang R, Zheng Y D and Ye J D 2019 *Chin. Phy. B* **28** 028501
[11] Shi Q, Wang Q R, Zhang D, Wang Q L, Li S H, Wang W J, Fan Q L and Zhang J Y 2019 *J. Lumin.* **206** 53
[12] Mazeina L, Picard Y N, Maximenko S I, Perkins F K, Glaser E R, Twigg M E, Freitas J A, Jr. and Prokes S M 2009 *Cryst. Growth Des.* **9** 4471
[13] Wu Z P, Bai G X, Qu Y Y, Guo D Y, Li L H, Li P G, Hao J H and Tang W H 2016 *Appl. Phys. Lett.* **108** 211903
[14] Vu T K, Lee D U and Kim E K 2019 *J. Alloys Compd.* **806** 874
[15] Liu H, Xu C X, Pan X H and Ye Z Z 2020 *J. Electron. Mater.* **49** 4544
[16] Berencén Y, Xie Y, Wang M, Prucnal S, Rebohle L and Zhou S Q 2019 *Semicond. Sci. Technol.* **34** 035001
[17] Feng Q, Li F G, Dai B, Jia Z T, Xie W L, Xu T, Lu X L, Tao X T, Zhang J C and Hao Y 2015 *Appl. Surf. Sci.* **359** 847
[18] Jangir R, Ganguli T, Porwal S, Tiwari P, Rai S K, Bhaumik I, Kukreja L M, Gupta P K and Deb S K 2013 *J. Appl. Phys.* **114** 074309
[19] Wang L 2016 *Scientist* **004** 163
[20] Chen X H, Han S, Lu Y M, Cao P J, Liu W J, Zeng Y X, Jia F, Xu W Y, Liu X K and Zhu D L 2018 *J. Alloys Compd.* **747** 869
[21] Lu Y M, Li C, Chen X H, Han S, Cao P J, Jia F, Zeng Y X, Liu X K, Xu W Y, Liu W J and Zhu D L 2019 *Chin. Phys. B* **28** 018504
[22] Zhang F B, Li H O, and Guo Q X 2018 *J. Electron. Mater.* **47** 6635
[23] Tak B R, Dewan S, Goyal A, Pathak R, Gupta V, Kapoor A K, Nagarajan S and Singh R 2019 *Appl. Surf. Sci.* **465** 973
[24] Guo D Y, Li P G, Chen Z W, Wu Z P and Tang W H 2019 *Acta Phys. Sin.* **68** 078501 (in Chinese)
[25] Kumar S S, Rubio E J, Noor-A-Alam M, Martinez G, Manandhar S, Shutthanandan V, Thevuthasan S and Ramana C V 2013 *J. Phys. Chem. C* **117** 4194
[26] Guo L, Shen X, Zhu G and Chen K 2011 *Sens. Actuators B Chem.* **155** 752
[27] Kneiß M, Hassa A, Splith D, Sturm C, Wenckstern H, Schultz T, Koch N, Lorenz M and Grundmann M 2019 *APL Mater.* **7** 022516
[28] Kim H, Horwitz J S, Pique A, Gilmore C M and Chrisey D B 1999 *Appl. Phys. A* **69** S447
[29] Heinemann M D, Berry J, Teeter G, Unold T and Ginley D 2016 *Appl. Phys. Lett.* **108** 013504
[30] Wu Z P, Bai G X, Hu Q R, Guo D Y, Sun C L, Ji L Y, Lei M, Li L H, Li P G, Hao J H and Tang W H 2015 *Appl. Phys. Lett.* **106** 171910
[31] Frodason Y K, Johansen K M, Vines and Varley J B 2020 *J. Appl. Phys.* **127** 075701
[32] Jiang J L, Zhang J and Song Z C 2020 *J. Lumin.* **221** 117048
[33] Mi W, Luan C N, Li Z, Zhao C S, Feng X J and Ma J 2013 *Opt. Mater.* **35** 2624
[34] Harwing T and Kellendouk F J. 1978 *Solid State Chem.* **24** 255
[35] Vasilotasiv V I, Zakharko Y M and Prim Y I 1988 *Ukr. Fiz. Zh.* **33** 1320
[36] Ho Q D, Frauenheim T and Deák P 2018 *Phys. Rev. B* **97** 115163
[37] Onuma T, Fujioka S, Yamaguchi T, Higashiwaki M, Sasaki K, Masui T and Honda T 2013 *Appl. Phys. Lett.* **103** 041910
[38] Binet L and Gourier D 1988 *J. Phys. Chem. Solids* **59** 1241